Article ID: 1000-7032(2013)09-1227-06

Optical Spectral Characteristics of Bragg Reflection Waveguide Lasers

WANG Li-jie[1,2], TONG Cun-zhu[1*], YANG Ye[1], ZENG Yu-gang[1], NING Yong-qiang[1], QIN Li[1], LIU Yun[1], WANG Li-jun[1]

(1. *State Key Laboratory of Luminescence and Application, Changchun Institute of Optics, Fine Mechanics and Physics, Chinese Academy of Sciences, Changchun* 130033, *China*;
2. *University of Chinese Academy of Sciences, Beijing* 100049, *China*)

* *Corresponding Author, E-mail: tongcz@ciomp.ac.cn*

Abstract: The continuous-wave single-mode operation of edge-emitting diode laser based on dual-sided non-quarter-wave Bragg reflection waveguide (BRW) was demonstrated at room temperature. A low-index core was utilized in the laser. The ridge BRW lasers (BRLs) exhibited an ultra-narrow twin-beam output. Single longitudinal mode emission with a very small spectral linewidth of 0.052 nm was measured. The lasing spectra showed a periodic modulation in the envelope with a mode spacing of approximately 3.3 nm. When the injection current of the BRLs was beyond 300 mA, a large mode hopping of the emission wavelength was observed.

Key words: Bragg reflection waveguide; diode laser; spectrum modulation
CLC number: TN248.4 **Document code:** A **DOI:** 10.3788/fgxb20133409.1227

布拉格反射波导激光器的光谱特性

汪丽杰[1,2], 佟存柱[1*], 杨 晔[1], 曾玉刚[1], 宁永强[1], 秦 莉[1], 刘 云[1], 王立军[1]

(1. 发光学及应用国家重点实验室 中国科学院长春光学精密机械与物理研究所, 吉林 长春 130033;
2. 中国科学院大学, 北京 100049)

摘要: 设计并制备了基于双边非1/4波长布拉格反射波导的边发射半导体激光器,中心腔采用低折射率材料,在垂直方向利用布拉格反射进行光限制,实现了超大光斑尺寸且稳定单横模工作。10 μm条宽、未镀膜的脊型激光器在准连续和连续工作方式下的总的输出功率分别超过了170 mW和80 mW,且最高功率受热扰动限制。激光器远场图案在垂直方向为双瓣状,单瓣垂直方向和水平方向发散角分别低至7.85°和6.7°。激射谱半高全宽仅为0.052 nm,光谱包络存在周期性调制现象,模式间隔约为3.3 nm。电流增加到300 mA以上时,激光器出现模式跳变。

关 键 词: 布拉格反射波导; 半导体激光器; 光谱调制

收稿日期: 2013-04-18; **修订日期:** 2013-07-11
基金项目: 国家自然科学基金(61076064,61176046); 中国科学院"百人计划"; 集成光电子学国家重点联合实验室开放课题(2011KFB006)资助项目
作者简介: 汪丽杰(1985-),男,河北石家庄人,博士研究生,主要从事高亮度半导体激光器方面的研究。
E-mail: wanglijie333@hotmail.com, Tel: (0431)86176335

1 Introduction

Diode lasers have been widely used in pumping solid-state lasers, material processing, medical treatment, sensing and printing applications. There is an increasing demand on power, divergence, linewidth and reliability of diode lasers in these applications. A key factor limiting high power operation of diode lasers is the catastrophic optical mirror damage (COMD), which can cause a sudden failure of laser chip due to the facet overheating resulted from the nonradiative surface recombination. An increase in the vertical spot size is helpful to reduce the optical power density and raise the power level where COMD occurs.

Many approaches have been reported to extend the optical mode distribution in the vertical direction, such as increasing the thickness of the waveguide layers [1-2], inserting low-index layer between the waveguide layer and cladding layer [3-4], or inserting additional high index layer into the low index cladding layer [5-6]. However, in these conventional total internal reflection waveguides, the significantly broadening waveguide still suffers from the presence of high order transverse modes, making the beam quality degraded. Although higher order modes could be suppressed by optical confinement factor and loss discrimination process by varying the claddings layer thickness or utilizing asymmetric waveguides [2,7], it is still difficult to achieve ultra-large modal spot size while maintaining single mode operation.

In order to overcome this problem, a novel type of lasers based on the Bragg reflection waveguide (BRW) or the so-called one-dimensional photonic crystal has been proposed [8]. The BRW is made up of a waveguide core sandwiched between two Bragg reflectors, and it uses Bragg reflection rather than traditional index-guiding to confine light in the direction perpendicular to the optical propagation direction. The BRW lasers (BRLs) possess a variety of advantages, including the high gain coefficient [9], large mode volumes [10], and strong mode discrimination [11-12], allowing for broad area and single mode operation. Another significant advantage of the BRL is that the waveguide core could have a lower index than the lowest index of the Bragg reflectors, which can exclude the index-guiding mechanism and achieve a much larger mode size [13]. In 2009, the first demonstration of an edge-emitting BRW laser with low index core in the vertical direction was reported [14], and further device characteristics were investigated in detail [15-16]. However, all of these previous reported devices were based on the quarter-wave BRWs (QtW-BRWs), in which the layer thickness of the periodic waveguides is a quarter-wave to the transverse propagation vector. In the QtW-BRWs, the guided mode is placed in the center of the photonic bandgap of the Bragg reflectors, which will maximize the confinement of optical field in the core. This tight confinement of light will restrict the optical mode expansion and lead to large vertical divergence.

In this paper, we demonstrated the continuous-wave single-mode operation of the BRL based on specially designed non-quarter-wave(non-QtW) BRW with low index core. The laser with 10 μm stripe width exhibits an ultra-narrow twin-lobed far field. Moreover, the detailed spectrum characteristics of the BRL were studied, which shows a very narrow spectral linewidth with subband emissions caused by spectrum modulation.

2 Laser Design and Fabrication

The schematic diagram of the BRL is shown in Fig. 1. It consists of a core layer sandwiched between the n-doped and p-doped distributed Bragg reflectors (DBR). The core layer has a refractive index n_c, serving as an optical defect layer. The active region is placed inside the core layer. The cladding DBR is made up of periodically alternated high and low index materials with indices n_1, n_2 respectively. When the propagation constant locates in within the photonic bandgap of the BRW, the optical field can be confined in the core layer even if the guided modes have the effective refractive indices n_{eff} lower than the lowest index n_2 in the DBR. The low-index core layer can ensure that the devices

operate at the BRW mode and not the total internal reflection mode. In addition, the modes arising from the BRW have large mode spacings and high loss difference between the fundamental mode and high-order modes, allowing for stable single transverse mode operation of BRLs.

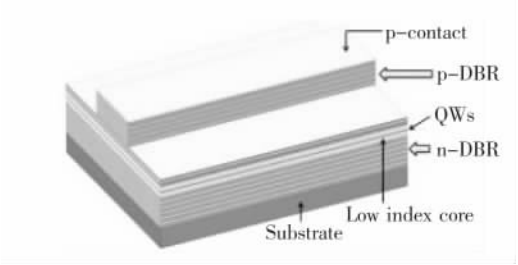

Fig. 1　Schematic diagram of the BRL

In this work, the designed BRL structure was based on a symmetric non-QtW BRW with low index core layer ($n_c = n_2$). It consists of 6 pairs $Al_{0.1}Ga_{0.9}As$/$Al_{0.3}Ga_{0.7}As$ top and bottom Bragg reflectors. The thickness of one pair was 100 nm/750 nm, respectively. The gain material was two 6-nm $In_{0.2}Ga_{0.8}As$ quantum wells (QWs) separated by 10-nm GaAs barrier, which was placed in the center of 1.5 μm thick $Al_{0.3}Ga_{0.7}As$ core layer. The total epitaxial thickness of the designed BRL is about 12.7 μm. All interfaces were linearly graded in composition over 20 nm to reduce the electrical resistance.

Fig. 2(a) shows the refractive index profile of the designed BRL structure. Fig. 2(b) illustrates the calculated near field distribution of the fundamental mode. As can be seen, the near field profile yields periodically oscillated peaks separated by nulls, and the peak intensities go down from the central to each side in nearly exponential evanescence. The transverse mode is extended throughout the entire width of the BRW, which can significantly reduce the power density and the far field divergence. The calculated far-field behavior in the vertical direction is shown in Fig. 2(c), which shows two pronounced lobes symmetrically located at about ±32°. The full width at half maximum (FWHM) of both lobes are respectively 6.36° and 6.54° in theory. This far field radiation pattern is determined by the Fourier transformation of the near field electric field distribution. For the near field with periodic local maxima and nulls, it can be approximate by a cosine function, which will result in a double-lobed far-field distribution.

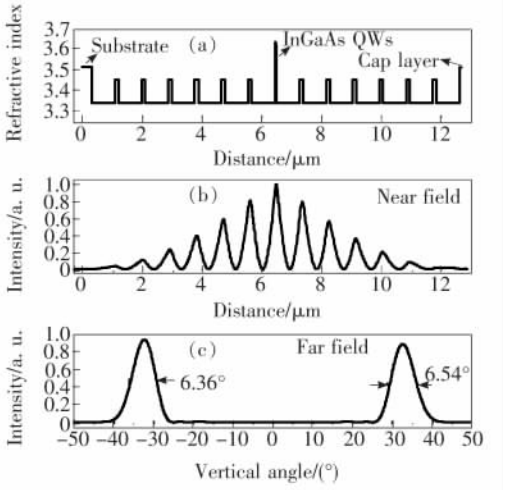

Fig. 2　Refractive index profile (a), calculated near field distribution (b), and calculated far field distribution (c) of the fundamental mode in the vertical direction of the BRL.

The laser structure was grown on n^+ GaAs (100)-oriented substrate by an Aixtron-200 metal-organic chemical vapor deposition (MOCVD) system. After the growth, ridge waveguides of 10 μm width were formed using conventional photolithography and wet etching. The etching depth was about 3 μm. Then 200 nm SiO_2 electrical insulating layer was deposited and contact window opening was done, followed by standard p-side metallization, substrate thinning and n-side metallization. Finally, individual ridge lasers with 1.4 mm cavity length were fabricated by cleaving the wafer without any facet passivation and coatings. The devices were tested without soldering and packaging.

3　Results and Discussion

3.1　Light-Current-Voltage Characteristics

Fig. 3 shows the light-current (*L-I*) curves of the uncoated ridge BRL with 10 μm width under continuous-wave (CW) and quasi-continuous-wave (QCW, pulse width = 200 μs, repetition rate = 1 kHz) operation at room temperature. As can be seen, in QCW mode an output power of 170 mW from two facets could be achieved without any sign of catastrophic optical damage. The CW output power

exceeds 84 mW from two facets, limited by the thermal roll-over. Higher output powers could be expected for devices soldering on the heatsink due to the better heat dissipation. The inset of Fig. 3 shows the temperature-dependence of the threshold current. As can be seen, the threshold current (I_{th}) increases from 125 mA to 220 mA when the temperature varies from 15 ℃ to 65 ℃. The corresponding characteristic temperature (T_0) in this temperature range is about 86 K.

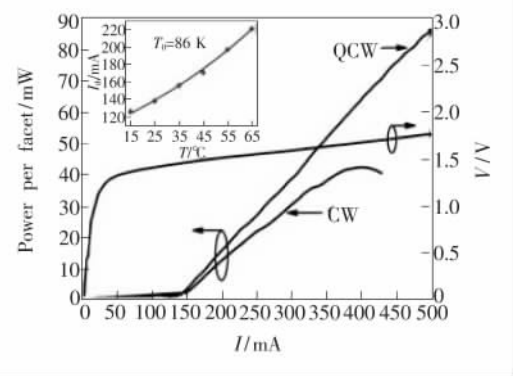

Fig. 3 Light-current (L-I) characteristics of the uncoated ridge BRL under CW and QCW operation (pulse width = 200 μs, repetition rate = 1 kHz) at room temperature, the top inset shows the temperature dependent threshold current.

3.2 Far-field Behavior

The measured far field distributions in the vertical and lateral direction at 400 mA are shown in Fig. 4. The most prominent feature is that the far field consists of two narrow lobes symmetrically located at about ±31° in the vertical direction. The vertical FWHM divergence angle of the upper and bottom lobes are respectively 7.85° and 9.1°, being in good agreement with the calculated results shown in Fig. 2(c). The intensity difference between these two lobes is because that the structure is not perfectly symmetric, one side is with the thick GaAs substrate and the other side is air. As shown in Fig. 4(b), the lateral far-field profile shows a clear Gaussian distribution with the FWHM divergence angle of 6.7°. This proves that the BRL enables fundamental lateral mode operation even for 10 μm wide ridge stripes, which is due to the ultra-thick vertical waveguide. The large vertical mode expansion will lead to weaker interaction of the optical field with the ridge edges and the active area, which could increase the stripe width for single lateral mode operation and suppress the generation of beam filamentation [17].

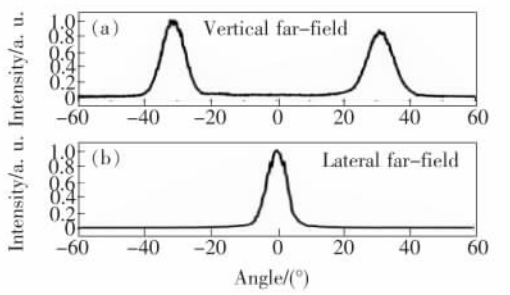

Fig. 4 Far-field profiles of the BRL in the vertical (a) and lateral(b) direction

In the previously reported QtW-BRWs laser, the tight confinement of light leads to very large vertical far-field divergence angle (>30° at FWHM for each lobe) and extremely strong power distribution in the central side-lobes. However, in our designed BRL based on non-QtW BRWs, nearly the entire emitted power is concentrated in the two ultra-narrow lobes, which shows a great improvement. This laser with narrow twin-beam output is in demand for a wide variety of applications, such as high speed laser scanning [18], high sensitivity laser absorption spectroscopy [19], and off-axis external cavity lasers [20]. For example, the dual-beam laser scanning can effectively improve the transfer rate of data limited by the rotation speed of the polygon scanner. Furthermore, the double well-correlated laser beams can also be used as signal and reference beams respectively in the laser absorption measurements, which can effectively reduce the intensity noise.

3.3 Spectrum Characteristics

The lasing spectra of the ridge BRLs were measured in CW operation by an ANDO AQ6317B optical spectrum analyzer. The spectrum of the laser at 420 mA injection current is shown in Fig. 5. As can be seen, the laser operates in a single longitudinal mode with spectral linewidth (FWHM, or the 3 dB linewidth) of 0.052 nm limited by the measurement resolution. The side mode suppression ratio (SMSR) is above 37 dB.

The detailed spectrum of the BRL at 280 mA is shown in Fig. 6. It can be observed that the BRL

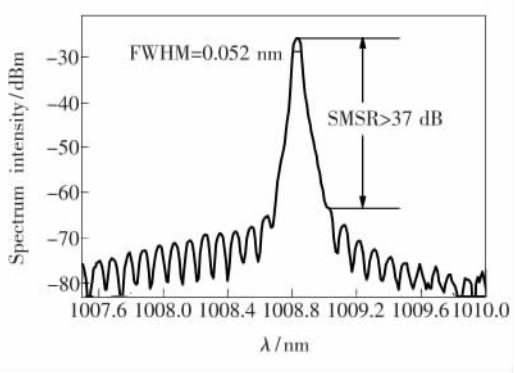

Fig. 5　Measured lasing spectrum of the ridge BRL at 420 mA injection current

exhibits a quite pronounced spectrum modulation superimposed on the normal longitudinal Fabry-Perot modes. Beside the main lasing wavelength of 1 002.79 nm, there are still four obvious peaks located at 996.04, 999.35, 1 006.08, 1 009.41 nm, respectively, indicating a uniform wavelength seperation of approximately 3.3 nm. This wavelength seperation of the sub-band emissions is one order of magnitude larger than the longitudinal mode spacing (~0.09 nm). In addition, the measured far-field distribution shown in Fig. 4 could exclude the possibility that this mode grouping effect is resulted from high order transverse modes or lateral modes, and the modulation period in the BRL is also not consistent with the 10 μm stripe width as in the lateral-cavity resonance case [21]. Therefore, we think that this periodic spectrum modulation should be due to the distributed reflection mechanism in the transverse BRW, which needs further investigation and theoretical analysis.

When the current increases to 360 mA, the mode with wavelength of 1 006.08 nm starts to reach threshold condition and dominate the lasing as shown in Fig. 7. This rapid switching of wavelength or so-called mode hopping is very similar to the DBR laser [22-23], which is caused by a thermal detuning of the gain and reflector sections. Increasing the injection current will change the temperature and the refractive index of the laser, which will influence the peak gain wavelength and maximum reflection wavelength of the BRW. The temperature dependence of these two parameters is different. Hence, the gain wavelength will shift slowly away from the reflection peak with changing temperature or current. But every time the mismatch between the two parameters reaches a certain value, the lasing wavelength may suddenly jump to the neighboring mode. During mode hopping, the laser's output power will fluctuate slightly, resulting in a kink in the *L-I* characteristics as shown in Fig. 3.

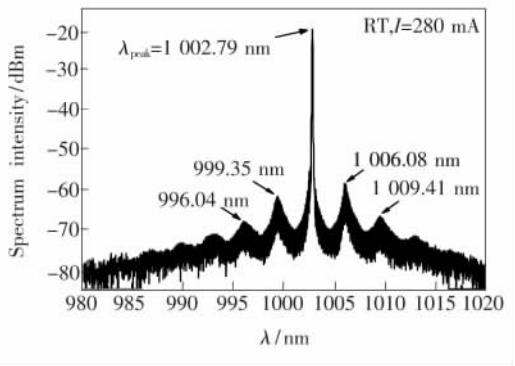

Fig. 6　Measured lasing spectrum of the ridge BRL at 280 mA

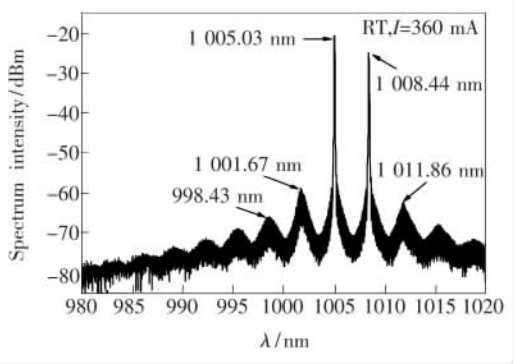

Fig. 7　Measured lasing spectrum of the ridge BRL at 360 mA injection current

4　Conclusion

In summary, we have demonstrated the CW and single mode operation of the dual-sided BRW diode laser. Nearly the entire emitted power of the BRL is concentrated in two lobes located at about ±31° in the vertical direction. The FWHM divergence angle of each lobe is as narrow as 7.85° and 6.7° respectively in the vertical and lateral directions. Lasing with a narrow spectrum linewidth of 0.052 nm is measured at 420 mA. The transverse Bragg reflection is shown to cause a periodic spectrum modulation with the mode spacing of 3.3 nm.

References:

[1] Pietrzak A, Wenzel H, Erbert G, *et al.* High-power laser diodes emitting light above 1 100 nm with a small vertical divergence angle of 13° [J]. *Opt. Lett.*, 2008, 33(19): 2188-2190.

[2] Pietrzak A, Wenzel H, Crump P, *et al.* 1 060-nm ridge waveguide lasers based on extremely wide waveguides for 1.3-W continuous-wave emission into a single mode with FWHM divergence angle of 9° × 6° [J]. *IEEE J. Quant. Elect.*, 2012, 48(5): 568-575.

[3] Malag A, Jasik A, Teodorczyk M, *et al.* High-power low vertical beam divergence 800-nm-band double-barrier-SCH GaAsP-(AlGa) as laser diodes [J]. *IEEE Photon. Technol. Lett.*, 2006, 18(15): 1582-1584.

[4] Hung C T, Lu T C. 830-nm AlGaAs-InGaAs graded index double barrier separate confinement heterostructures laser diodes with improved temperature and divergence characteristics [J]. *IEEE J. Quant. Elect.*, 2013, 49(1): 127-132.

[5] Chen Y C, Waters R G, Dalby R J. Single-quantum-well laser with 11.2 degree transverse beam divergence [J]. *Electron. Lett.*, 1990, 26(17): 1348-1350.

[6] Wenzel H, Bugge F, Erbert G, *et al.* High-power diode lasers with small vertical beam divergence emitting at 808 nm [J]. *Elect. Lett.*, 2001, 37(16): 1024-1026.

[7] Malag A, Dabrowska E, Teodorczyk M, *et al.* Asymmetric heterostructure with reduced distance from active region to heat-sink for 810-nm range high-power laser diodes [J]. *IEEE J. Quant. Elect.*, 2012, 48(4): 465-471.

[8] Liang W, Xu Y, Choi J M, *et al.* Engineering transverse Bragg resonance waveguides for large modal volume lasers [J]. *Opt. Lett.*, 2003, 28(21): 2079-2081.

[9] Yariv A, Xu Y, Mookherjea S. Transverse Bragg resonance laser amplifier [J]. *Opt. Lett.*, 2003, 28(3): 176-178.

[10] Her T H. Gain-guiding in transverse grating waveguides for large modal area laser amplifiers [J]. *Opt. Exp.*, 2008, 16(10): 7197-7202.

[11] Zhu L, Scherer A, Yariv A. Modal gain analysis of transverse Bragg resonance waveguide lasers with and without transverse defects [J]. *IEEE J. Quant. Elect.*, 2007, 43(10): 934-940.

[12] Tao M M, Yang P L, Liu W P, *et al.* Response characteristics of fiber Bragg gratings irradiated by high energy lasers [J]. *Chin. Opt.* (中国光学), 2012, (5): 544-549 (in Chinese).

[13] Cregan R F, Mangan B J, Knight J C, *et al.* Single-mode photonic band gap guidance of light in air [J]. *Science*, 1999, 285(5433): 1537-1539.

[14] Bijlani B J, Helmy A S. Bragg reflection waveguide diode lasers [J]. *Opt. Lett.*, 2009, 34(23): 3734-3736.

[15] Tong C Z, Bijlani B J, Alali S, *et al.* Characteristics of edge emitting Bragg reflection waveguide lasers [J]. *IEEE J. Quant. Elect.*, 2010, 46(11): 1605-1610.

[16] Tong C Z, Bijlani B J, Zhao L J, *et al.* Mode selectivity in bragg reflection waveguide lasers [J]. *IEEE Photon. Technol. Lett.*, 2011, 23(14): 1025-1027.

[17] Maximov M V, Shernyakov Y M, Novikov I I, *et al.* High-power low-beam divergence edge-emitting semiconductor lasers with 1- and 2-D photonic bandgap crystal waveguide [J]. *IEEE J. Select. Topics Quant. Elect.*, 2008, 14(4): 1113-1122.

[18] Kataoka K. Analysis of banding problem in multiple beam scanning system of laser printer [J]. *Opt. Rev.*, 2008, 15(4): 196-203.

[19] Heidmann A, Horowicz R J, Reynaud S, *et al.* Observation of quantum noise reduction on twin laser beams [J]. *Phys. Rev. Lett.*, 1987, 59(22): 2555-2557.

[20] Jechow A, Lichtner M, Menzel R, *et al.* Stripe-array diode-laser in an off-axis external cavity: Theory and experiment [J]. *Opt. Exp.*, 2009, 17(22): 19599-19604.

[21] Ouyang D, Heitz R, Ledentsov N N, *et al.* Lateral-cavity spectral hole burning in quantum-dot lasers [J]. *Appl. Phys. Lett.*, 2002, 81(9): 1546-1548.

[22] Fricke J, Wenzel H, Matalla M, *et al.* 980-nm DBR lasers using higher order gratings defined by i-line lithography [J]. *Semicond. Sci. Technol.*, 2005, 20(11): 1149-1152.

[23] Feise D, John W, Bugge F, *et al.* 96 mW longitudinal single mode red-emitting distributed Bragg reflector ridge waveguide laser with tenth order surface grating [J]. *Opt. Lett.*, 2012, 37(9): 1532-1534.